

## Fundamental optical transitions in GaN

G. D. Chen, M. Smith, J. Y. Lin, H. X. Jiang, SuHuai Wei, M. Asif Khan, and C. J. Sun

Citation: *Applied Physics Letters* **68**, 2784 (1996); doi: 10.1063/1.116606

View online: <http://dx.doi.org/10.1063/1.116606>

View Table of Contents: <http://scitation.aip.org/content/aip/journal/apl/68/20?ver=pdfcov>

Published by the [AIP Publishing](#)

## Instruments for advanced science

### Gas Analysis



- dynamic measurement of reaction gas streams
- catalysis and thermal analysis
- molecular beam studies
- dissolved species probes
- fermentation, environmental and ecological studies

### Surface Science



- UHV TPD
- SIMS
- end point detection in ion beam etch
- elemental imaging - surface mapping

### Plasma Diagnostics



- plasma source characterization
- etch and deposition process
- reaction kinetic studies
- analysis of neutral and radical species

### Vacuum Analysis



- partial pressure measurement and control of process gases
- reactive sputter process control
- vacuum diagnostics
- vacuum coating process monitoring

contact Hiden Analytical for further details

**HIDEN**  
ANALYTICAL

[info@hideninc.com](mailto:info@hideninc.com)  
[www.HidenAnalytical.com](http://www.HidenAnalytical.com)

CLICK to view our product catalogue



# Fundamental optical transitions in GaN

G. D. Chen,<sup>a)</sup> M. Smith, J. Y. Lin, and H. X. Jiang  
Department of Physics, Kansas State University, Manhattan, Kansas 66506-2601

Su-Huai Wei  
National Renewable Energy Laboratory, Golden, Colorado 80401-3393

M. Asif Khan and C. J. Sun  
APA Optics, Inc., 2950 N.E. 84th Lane, Blaine, Minnesota 55449

(Received 2 January 1996; accepted for publication 8 March 1996)

A coherent picture for the band structure near the  $\Gamma$  point and the associated fundamental optical transitions in wurtzite (WZ) GaN, including the electron and hole effective masses and the binding energies of the free excitons associated with different valence bands, has been derived from time-resolved photoluminescence measurements and a theoretical calculation based on the local density approximation. We also determine the radiative recombination lifetimes of the free excitons and neutral impurity (donor and acceptor) bound excitons in WZ GaN and compare ratios of the radiative lifetimes with calculated values of the ratios obtained with existing theories of free and bound excitons. © 1996 American Institute of Physics. [S0003-6951(96)02220-6]

GaN has been recognized as one of the most important wide-band-gap semiconductors recently due to its potential applications for optical devices such as blue-UV lasers and for high-temperature electronic devices.<sup>1,2</sup> In spite of the recognition of the importance of GaN, many of its fundamental physical properties are not yet well known. For example, key parameters which describe the band structure near the  $\Gamma$  point, including the values of the valence band splitting and the hole effective masses, are not well established. In this letter, we present a coherent picture for the fundamental optical transitions and the detailed band structures near the  $\Gamma$  point in GaN, derived from time-resolved photoluminescence measurements and a first-principles band structure calculation based on the local density approximation (LDA).

Three GaN samples grown by metalorganic chemical vapor deposition (MOCVD) were used in this study: Sample A is a 3.8  $\mu\text{m}$   $n$ -type ( $n=5\times 10^{16}\text{ cm}^{-3}$ ) epitaxial layer; sample B is a 2.8  $\mu\text{m}$   $n$ -type ( $n=2.4\times 10^{17}\text{ cm}^{-3}$ ) epitaxial layer; and sample C is a 0.2  $\mu\text{m}$   $p$ -type (Mg-doped) epitaxial layer. All layers were grown on sapphire substrates with AlN buffer layers.<sup>3,4</sup> The picosecond laser spectroscopy system used for time-resolved photoluminescence measurements has been described previously.<sup>3</sup>

Figure 1 shows three low-temperature photoluminescence emission spectra obtained for samples A, B, and C. The spectral peak positions shift with temperature following the temperature variation of the band gap. Two emission peaks located at about 3.485 and 3.491 eV observed in sample A are identified as due to the recombination of the ground state of free excitons (FX) associated with the top two valence bands, or  $A$  and  $B$  excitons [ $A(n=1)$  and  $B(n=1)$ ]. These assignments have been further confirmed by the following three observations: (a) the emission intensities of the observed transition lines decrease with temperature with activation energies correspond to FX binding energies; (b)

the emission intensities depend strongly on the excitation light polarization direction, as expected for FX in WZ crystals; and (3) the emission intensities increase superlinearly with excitation intensity, as expected for FX. Our results show that the energy separation between the  $A$ - and  $B$ -exciton transition lines is about 6 meV; the binding energy of the  $A$  exciton is about 19 meV if we use the accepted value of the low-temperature band gap of 3.504 eV.<sup>5-7</sup> We show the 40 K emission spectrum for sample A because the  $B$ -exciton line is more pronounced at  $T\leq 40$  K in sample A. An emission line due to the recombination of the first excited state of the  $A$ -exciton  $A(n=2)$ , which is about 14.3 meV above the  $A(n=1)$  emission line, is also observable in sample A at  $T>40$  K. These values are in agreement with those obtained recently for GaN grown by molecular beam epitaxy (MBE).<sup>5,6</sup>

The dominant transition line at 3.476 eV observed in

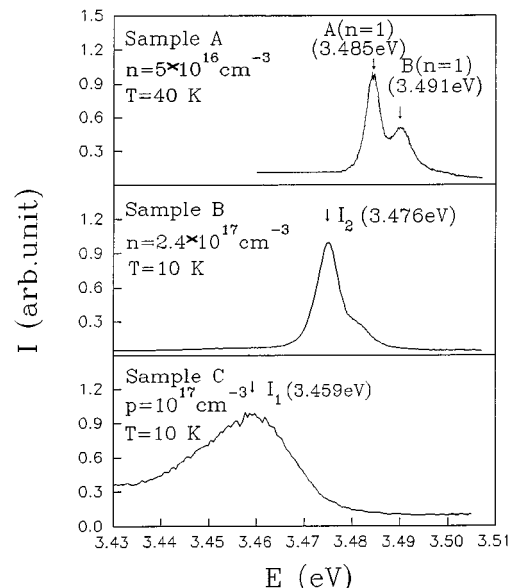


FIG. 1. Low-temperature cw photoluminescence spectra of GaN for three different MOCVD samples. The arrows indicate the dominant transition peaks for each sample.

<sup>a)</sup>Permanent address: Department of Applied Physics, Xi'an Jiaotong University, People's Republic of China.

TABLE I. Structural and band parameters of wurtzite GaN calculated by LDA.

Lattice constant (Å)	Internal parameter ( $u^a$ )	Energy split (meV)				Effective mass in $m_0$		Density of state mass ( $m_0$ ) <sup>b</sup>	Exciton parameters	
		Crystal field	Spin-orbit	$\Delta E_{AB}$	$\Delta E_{AC}$	$\parallel$	$\perp$		$m_r(m_0)^c$	$E_b(\text{meV})^d$
$a=3.1699$						$m_e=0.17$	$m_e=0.19$	$m_e=0.18$	0.13	20 A
$c/a=1.6250$	0.377	37.5	12	6	43	$m_h^A=2.03$	$m_h^A=0.33$	$m_h^A=0.60$	0.13	20 B
						$m_h^B=1.25$	$m_h^B=0.34$	$m_h^B=0.52$	0.12	18 C
						$m_h^C=0.15$	$m_h^C=1.22$	$m_h^C=0.61$		

<sup>a</sup>Internal parameter  $u$  is the nearest-neighbor distance between Ga and N atoms along the  $c$ -axis in unit of the lattice constant  $c$ .

<sup>b</sup>Density of state effective mass is evaluated according to  $m^*=(m_{\parallel}m_{\perp}^2)^{1/3}$ .

<sup>c</sup>Exciton reduced mass is calculated using  $m_r=[(2/3)(1/m_r^{\perp})+(1/3)(1/m_r^{\parallel})]^{-1}$ , where  $m_r^{\perp}=(1/m_e^{\perp}+1/m_h^{\perp})^{-1}$  and  $m_r^{\parallel}=(1/m_e^{\parallel}+1/m_h^{\parallel})^{-1}$ .

<sup>d</sup>The low-frequency dielectric constant  $\epsilon=9.5$  has been used to calculate the exciton binding energies  $E_b$ .

sample B, the  $I_2$  line, is due to the recombination of the excitons bound to neutral donors associated with nitrogen vacancies. The shoulder at about 3.484 eV in sample B is due to the free exciton  $A(n=1)$  recombination. We thus obtain a value between 8–9 meV for the binding energy of the neutral-donor-bound exciton. The transition line at 3.459 eV (the  $I_1$  line) observed in sample C is due to the recombination of the excitons bound to neutral acceptors associated with Mg impurities. A value of about 25 meV is obtained for the binding energy of the acceptor-bound exciton.

In order to obtain the detailed band structure parameters near the  $\Gamma$  point, we have performed first-principles band structure calculations for WZ GaN using local density approximation (LDA) as implemented by the all-electron, relativistic, full-potential linearized augmented plane wave (FLAPW) method.<sup>8</sup> Band parameters near the  $\Gamma$  point are calculated at the equilibrium lattice constants, which are determined by minimizing the total energy. The calculated results are listed in Table I. The calculated lattice constant  $a$  and the ratio of  $c/a$  are in good agreement with the experimental values<sup>9,10</sup> and with other calculations.<sup>11,12</sup> The calculated three energy levels of the top valence bands at the  $\Gamma$  point are fitted to the quasicubic model of Hopfield<sup>13</sup> to extract the spin-orbit splitting  $\Delta_{SO}$  and crystal-field splitting  $\Delta_{CF}$ . Both values are found to be positive for GaN. We notice that although  $\Delta_{SO}$  is insensitive to the structural parameters,  $\Delta_{CF}$  is very sensitive to the ratio  $\eta=c/a$  and the internal structural parameter  $u(d\Delta_{CF}/d\eta=2.02$  eV and  $d\Delta_{CF}/du=-17.0$  eV). To confirm our calculation, we have also performed a parallel band structure calculation for the well-understood WZ CdS, which has a band structure similar to GaN. The obtained  $\Delta_{SO}=55$  meV and  $\Delta_{CF}=47$  meV for CdS agree well with experimental values.<sup>13,14</sup> The effective masses of electrons and holes are obtained by calculating the second derivative of the energy dispersion curves near  $\Gamma$ . The energy bands show considerable nonparabolic behavior. This is especially true for the valence bands, which also show spin splitting in the direction perpendicular to the  $c$  axis due to the lack of inversion symmetry of WZ structure. The effective masses of electrons and holes given in Table I are obtained by averaging over the spin-split states. Since the LDA calculation underestimates the band gap, our calculated effective masses are expected to be slightly lower than the actual values. The calculated electron effective masses for  $m_{e\parallel}=0.17m_0$  and  $m_{e\perp}=0.19m_0$  can be compared with the experimental values of  $m_{e\parallel}\approx m_{e\perp}\approx 0.2m_0$ ,<sup>7</sup> suggesting the

calculation underestimates these values by about 10–20%.

By using a value of  $\epsilon=9.5$  for the low-frequency dielectric constant of GaN and our calculated effective masses, the binding energies of  $A$ ,  $B$ , and  $C$  excitons are calculated to be 20, 20, and 18 meV, respectively, also shown in Table I and Fig. 2. The calculated  $A$ -exciton binding energy agrees very well with our experimental results. The near coincidence of the three exciton binding energies is due to the fact that the exciton reduced masses are predominantly determined by the electron mass because of the heavier hole masses. This is similar to the case in the WZ CdS in which the binding energies of the  $A$ - and  $B$ -excitons,  $E_A^b$  and  $E_B^b$ , are the same and the binding energy of the  $C$  exciton has a slightly lower value,  $E_C^b=0.915 E_A^b$  ( $E_C^b=0.91E_A^b$  for GaN). Therefore the calculated energy difference between the  $A$  and  $B$  valence bands ( $\Delta E_{AB}=6$  meV) should be close to the energy separation observed between the  $A$ - and  $B$ -exciton transition peaks, which is confirmed by our experimental data obtained for sample A shown in Fig. 1 ( $E_{A(n=1)} - E_{B(n=1)}=6$  meV). The calculated energy splitting between the  $A$  and  $C$  valence bands,  $\Delta E_{AC}$  is 43 meV.

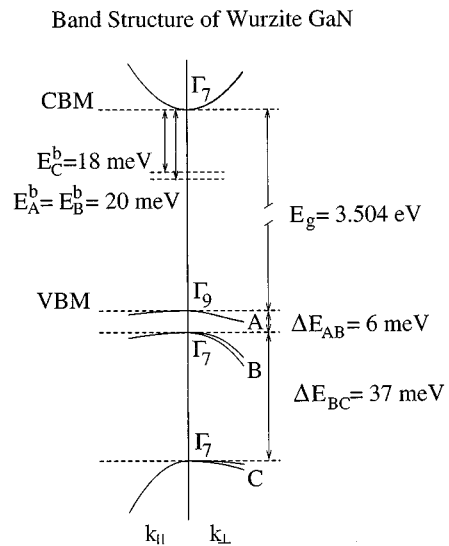


FIG. 2. Calculated band structure near the  $\Gamma$  point of WZ GaN. At  $k=0$ , the top of the valence band is split by crystal field and spin orbit coupling into the  $A(\Gamma_9)$ ,  $B(\Gamma_7)$ , and  $C(\Gamma_7)$  states. The conduction band is shifted upwards so that the band gap agrees with experiment. The exciton binding energies are denoted as  $E_A^b$ ,  $E_B^b$ ,  $E_C^b$  for the  $A$ ,  $B$ , and  $C$  excitons, respectively.

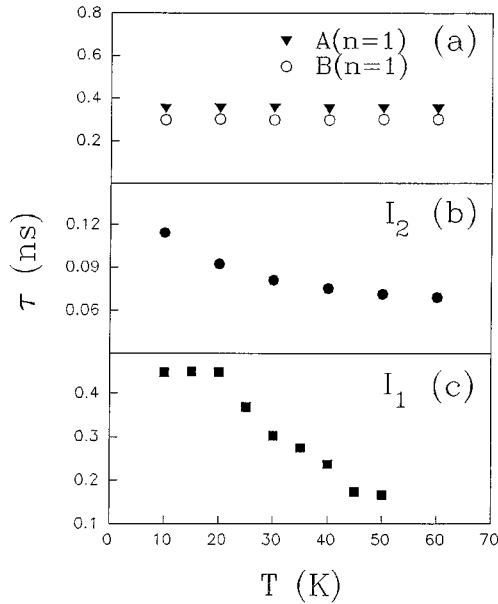


FIG. 3. Temperature dependence of the recombination lifetime of the (a) A- and B-exciton, (b)  $I_2$ , and (c)  $I_1$  transitions measured at their corresponding spectral peak positions and low excitation power densities.

Based on our experimental results and theoretical calculations, a band diagram near the  $\Gamma$  point of WZ GaN is obtained and shown in Fig. 2.

The dynamical behavior of the free- and impurity-bound excitons has also been studied. The decays of the excitonic transitions in samples investigated here are described well by a single-exponential form,  $I(t) = I_0 \exp(-t/\tau)$ . The temperature dependencies of the recombination lifetime ( $\tau$ ) of the A-exciton, B-exciton,  $I_2$ , and  $I_1$  transitions measured at low excitation power densities are plotted in Fig. 3. The measured recombination lifetimes of the A exciton ( $\sim 0.35$  ns) and B exciton ( $\sim 0.30$  ns) transition are nearly temperature independent, which indicates that the recombination is dominated by radiative processes in sample A. We have calculated the square of the transition matrix element,  $I_v = |\langle \psi_V | H_{\text{dipole}} | \psi_C \rangle|^2$ , for the band-to-band transition involving the three valence bands using the quasicubic model,<sup>13</sup> which correlates directly to the radiative lifetimes of the band-to-band recombination. Here,  $\Psi_V$  and  $\Psi_C$  are the electron and hole wave functions. The calculated values of  $I_v$  for the three A-, B-, and C-valence band to conduction band transitions at two different excitation light polarizations,  $\mathbf{E} \parallel c$  and  $\mathbf{E} \perp c$ , are listed in Table II. Our results indicate that for the case  $\mathbf{E} \perp c$ , the values of  $I_v$  are about the same for band-to-band transitions involving the A- and B-valence bands (1 vs 0.974). Since the reduced masses and hence the effective Bohr radii of the A and B excitons are comparable, we expect the radiative recombination lifetimes of the A and B excitons to be close in the  $\mathbf{E} \perp c$  configuration, which is consistent with our experimental observation.

The radiative recombination lifetimes of the  $I_2$  and  $I_1$  transitions can be obtained by extrapolating the plots in Figs. 3(b) and 3(c) to  $T=0$ , which is about 0.13 and 0.45 ns, respectively. The relation between the oscillator strength of the impurity-bound exciton  $F$  and of the free excitons  $F_{\text{ex}}$  has been obtained previously as<sup>15</sup>

TABLE II. Calculated relative square of the transition dipole matrix element  $I_v$  of WZ GaN for lights polarized parallel and perpendicular to the  $c$  axis.

Transition	$\mathbf{E} \parallel c$	$\mathbf{E} \perp c$
$E_A(\Gamma_{7C} \leftrightarrow \Gamma_{9V})$	0	1
$E_B(\Gamma_{7C} \leftrightarrow \Gamma_{7V})$	0.053	0.974
$E_C(\Gamma_{7C} \leftrightarrow \Gamma_{7V})$	1.947	0.026

$$F = (E_0/E_i)^{3/2} F_{\text{ex}}. \quad (1)$$

Here,  $E_i$  is the binding energy of the impurity-bound excitons,  $E_0 = (2\hbar^2/m)(\pi/\Omega_0)^{2/3}$ ,  $m$  is the effective mass of the intrinsic exciton, and  $\Omega_0$  is the volume of the unit cell. From Eq. (1), we thus have the ratio of radiative decay lifetimes  $I_1$  and  $I_2$  as

$$\tau(I_1)/\tau(I_2) = F(I_2)/F(I_1) = [E(I_1)/E(I_2)]^{3/2}. \quad (2)$$

From Eq. (2), we obtain  $\tau(I_1)/\tau(I_2) = 5$  by taking the binding energies of the neutral-acceptor- and neutral-donor-bound excitons from our results,  $E(I_1) = 25$  and  $E(I_2) = 8.5$  meV. Our measured ratio  $\tau(I_1)/\tau(I_2)$  is 3.5, which is in fair agreement with Eq. (2) considering the fact that both  $\tau(I_1)$  and  $\tau(I_2)$  depend on emission energy.

In conclusion, a fairly complete picture for the band structure near the  $\Gamma$  point and the associated fundamental optical transitions in GaN has been derived from time-resolved photoluminescence measurements and from a first-principles band structure calculation based on the local density approximation. The electron and hole effective masses have been obtained. The binding energies of about 20 meV for the A and B excitons, 18 meV for the C excitons, 8.5 meV for the neutral-donor bound exciton, and 25 meV for the neutral-acceptor bound exciton have been obtained. Radiative recombination lifetimes of about 0.35 ns for the free excitons, 0.13 ns for the neutral-donor-bound exciton, and 0.45 ns for the neutral-acceptor-bound exciton have been observed and compared with theoretical calculations.

J. Y. Lin and H. X. Jiang would like to acknowledge insightful discussions and support of Dr. John Zavada.

<sup>1</sup>H. Morkoç, S. Strite, G. B. Gao, M. E. Lin, B. Sverdlov, and M. Burns, *J. Appl. Phys.* **76**, 1363 (1994).

<sup>2</sup>M. Asif Khan, M. S. Shur, J. N. Kuznia, Q. Chen, J. Burm, and W. Schaff, *Appl. Phys. Lett.* **66**, 1083 (1995).

<sup>3</sup>G. D. Chen, M. Smith, J. Y. Lin, H. X. Jiang, M. A. Khan, and C. J. Sun, *Appl. Phys. Lett.* **67**, 1653 (1995); M. Smith, G. D. Chen, J. Y. Lin, H. X. Jiang, M. A. Khan, and C. J. Sun, *Appl. Phys. Lett.* **67**, 3295 (1995).

<sup>4</sup>M. A. Khan, Fall Meeting of MRS, Boston MA, November, 1995.

<sup>5</sup>M. Smith, G. D. Chen, J. Y. Lin, H. X. Jiang, A. Salvador, W. K. Kim, O. Aktas, A. Botchkarev, and H. Morkoç, *Appl. Phys. Lett.* **67**, 3387 (1995).

<sup>6</sup>D. C. Reynolds, D. C. Look, W. K. Kim, O. Aktas, A. Botchkarev, A. Salvador, and H. Morkoç (unpublished).

<sup>7</sup>Landolt-Börnstein, *Numerical Data and Functional Relationships in Science and Technology*, edited by P. Eckerlin and H. Kandler (Springer-Verlag, Berlin, 1971), Vol. III.

<sup>8</sup>S. H. Wei and A. Zunger, *Appl. Phys. Lett.* **64**, 1676 (1994).

<sup>9</sup>H. P. Maruska and J. J. Tietjen, *Appl. Phys. Lett.* **15**, 327 (1969).

<sup>10</sup>H. Schulz and K. H. Thiemann, *Solid State Commun.* **23**, 815 (1977).

<sup>11</sup>K. Miwa and A. Fukumoto, *Phys. Rev. B* **48**, 7897 (1993).

<sup>12</sup>A. F. Wright and J. S. Nelson, *Phys. Rev. B* **50**, 2159 (1994).

<sup>13</sup>J. J. Hopfield, *J. Phys. Chem. Solids* **15**, 97 (1960).

<sup>14</sup>D. G. Thomas and J. J. Hopfield, *Phys. Rev.* **103**, 1715 (1956).

<sup>15</sup>E. I. Rashba and G. E. Gurgenishvili, *Fiz. Tverd. Tela* **4**, 1029 (1962) [*Sov. Phys.-Solid State* **4**, 759 (1962)].